

This work was written as part of one of the author's official duties as an Employee of the United States Government and is therefore a work of the United States Government. In accordance with 17 U.S.C. 105, no copyright protection is available for such works under U.S. Law.

Public Domain Mark 1.0

<https://creativecommons.org/publicdomain/mark/1.0/>

Access to this work was provided by the University of Maryland, Baltimore County (UMBC) ScholarWorks@UMBC digital repository on the Maryland Shared Open Access (MD-SOAR) platform.

Please provide feedback

Please support the ScholarWorks@UMBC repository by emailing scholarworks-group@umbc.edu and telling us what having access to this work means to you and why it's important to you. Thank you.

Mean Profiles of Trace Reactive Species in the Unpolluted Marine Surface Layer

ANNE M. THOMPSON AND DONALD H. LENSCHOW

National Center for Atmospheric Research

We have investigated several aspects of trace gas photochemistry in the marine boundary layer using a time-dependent transport-kinetics model with one-dimensional eddy diffusion. The photochemical scheme in the model (Thompson and Cicerone, 1982) is represented by a conventional complement of reactions involving O, H, N, and methane-derived organic species; boundary conditions are assigned which give low surface mixing ratios of O₃ and NO_x (Routhier et al., 1980; McFarland et al., 1979) characteristic of the remote marine environment. Altitude dependent eddy diffusion coefficients in the surface layer (1 mm to 100 m) are based on the formulation of Businger et al. (1971) for temperature diffusivity in an unstably stratified surface layer. Diffusion coefficients in the rest of the convective boundary layer (the mixed layer) are taken from Lamb and Durran (1978). The surface is assumed to be the tropical ocean with a steady state mixed layer. In the simulations described here, particular attention has been given to the distribution of odd nitrogen and the NO₂-NO-O₃ photostationary state in the surface boundary layer. Calculated profiles of NO, NO₂, O₃, and HNO₃ show definite gradients in the surface layer. When the ocean is assumed to be a source of NO, mixing ratios on the order of a few parts per trillion can be supported by an upflux of $\sim 10^8 \text{ cm}^{-2} \text{ s}^{-1}$. If a surface input of NO is not assumed, NO_x levels are much lower. This is consistent with measurements in the Equatorial Pacific (McFarland et al., 1979; Zafriou et al., 1980; Liu et al., 1983) and suggests that NO upwelling may be significant in the local budget of NO_x in certain remote marine environments. Calculated values of the O₃-NO-NO₂ photostationary state ratio, R_{ps} , and NO/HNO₃ show appreciable variation within the surface layer. The latter ratio is sensitive to the NO upflux and to heterogeneous removal of HNO₃. R_{ps} decreases away from the surface and is unity only at one point. Both chemical and micrometeorological factors (Lenschow, 1982) contribute to nonunity values of R_{ps} . Significant departures from a profile characteristic of a nonreactive species are shown to occur in the NO profile as low as 0.2 m above the surface.

1. INTRODUCTION

Trace gases in the boundary layer are subject to various micrometeorological and physicochemical influences. In the surface layer (the lowest few meters of the boundary layer where the fluxes of conserved species can be considered constant) turbulent mixing on a rapid time scale can upset the photochemical equilibrium relations among reactive trace gases [Lenschow, 1982; Fitzjarrald and Lenschow, 1983]. In this same region, heterogeneous effects—the interaction of certain gases with aerosols, fog, and falling rain and snow—can also disrupt simple photochemistry. The result is a high degree of variability in boundary layer trace gas distribution on small time and space scales.

We have reported previously on certain aspects of this variability in modeling studies of the remote marine troposphere [Thompson and Cicerone, 1982; Thompson and Zafriou, 1983]. Using a one-dimensional photochemical-transport model with a moderately refined boundary layer (minimum vertical resolution = 6.25 m), we demonstrated that near-surface mixing ratios of NO_x (NO_x = NO + NO₂) and soluble gases like HNO₃, H₂O₂, and CH₃OOH are very sensitive to surface fluxes, heterogeneous removal, and near-surface eddy diffusion rates. The purpose of the present investigation is to focus in more detail on a few of these processes, specifically to examine with a model the chemical fine structure in the lowest 100 m of the atmosphere, where ground, tower, and ship-based measurements of chemical concentrations are obtained.

In particular we simulate conditions typical of a suppressed marine trade wind regime. Although disturbed synoptic situations are potentially important for large-scale exchange be-

tween the boundary layer and the free troposphere [Chatfield and Crutzen, 1984; Gidel, 1983], as well as for lightning-produced NO_x [Noxon, 1976; Chameides et al., 1977], they are not included in this study because their effects on the boundary layer are more difficult to quantify. We also look at the chemical composition in the rest of the convective boundary layer (i.e., the mixed layer above the surface layer) where mixing times and the photochemical reaction times considered here are comparable and a state closer to photochemical equilibrium is predicted theoretically [Lenschow, 1982].

Our model is described in section 2. Basic chemical and transport features are the same as in Thompson and Cicerone [1982], but in the present set of simulations the altitude grid has been compressed and refined. We have also introduced a simplified eddy-diffusion treatment that represents mixing in the tropical marine boundary layer. Section 3 summarizes results of typical species diurnal cycles obtained from the modified transport scheme. We also report findings from a series of model sensitivity runs designed to look closely at the odd nitrogen system in the surface layer. Here we have been motivated by several concerns: (1) the role of an oceanic NO source [Zafriou and McFarland, 1981] in determining boundary layer NO_x; (2) the effects of heterogeneous removal and ocean-derived NO on the NO/HNO₃ ratio; (3) the structure of the NO-O₃-NO₂ photostationary state ratio in the surface layer, where considerable structure and deviation from unity have been predicted [Fitzjarrald and Lenschow, 1983; Calvert and Stockwell, 1983].

2. MODEL DESCRIPTION

Chemical Kinetics

Chemical distributions of trace gases are determined as a function of altitude from a system of one-dimensional

Copyright 1984 by the American Geophysical Union.

Paper number 4D0313.
0148-0227/84/004D-0313\$05.00

TABLE 1. Fixed Parameters and Eddy Coefficients for Model Troposphere

Altitude, m	Temperature, K	Molecular Density,* $N(\times 10^{19} \text{ cm}^{-3})$	Eddy Diffusion Coefficient, $K, \text{ cm}^2 \text{ s}^{-1}$	H ₂ O Mixing† Ratio	CO Mixing Ratio
1000.0	294.4	2.212	1.680(4)‡	2.11(−3)	1.18(−7)
464.16	298.9	2.274	7.067(5)	3.32(−2)	1.19(−7)
215.44	301.5	2.337	7.067(5)	3.32(−2)	1.20(−7)
100.00	302.1	2.402	4.000(5)	3.32(−2)	1.20(−7)
5.6234(1)	302.3	2.407	2.046(5)	3.32(−2)	1.20(−7)
3.1623(1)	302.4	2.412	8.756(4)	3.32(−2)	1.20(−7)
1.7783(1)	302.5	2.417	3.785(4)	3.32(−2)	1.20(−7)
1.0000(1)	302.6	2.422	1.664(4)	3.32(−2)	1.20(−7)
5.6234	302.6	2.423	7.496(3)	3.32(−2)	1.20(−7)
3.1623	302.6	2.423	3.492(3)	3.32(−2)	1.20(−7)
1.7783	302.6	2.424	1.693(3)	3.32(−2)	1.20(−7)
1.0000	302.6	2.425	8.543(2)	3.32(−2)	1.20(−7)
5.6234(−1)	302.6	2.425	4.466(2)	3.32(−2)	1.20(−7)
3.1623(−1)	302.6	2.425	2.398(2)	3.32(−2)	1.20(−7)
1.7783(−1)	302.6	2.425	1.311(2)	3.32(−2)	1.20(−7)
1.0000(−1)	302.6	2.425	7.252(1)	3.32(−2)	1.20(−7)
5.6234(−2)	302.6	2.425	4.040(1)	3.32(−2)	1.20(−7)
3.1623(−2)	302.6	2.425	2.259(1)	3.32(−2)	1.20(−7)
1.7783(−2)	302.6	2.425	1.267(1)	3.32(−2)	1.20(−7)
1.0000(−2)	302.6	2.425	7.111	3.32(−2)	1.20(−7)
5.6234(−3)	302.6	2.425	3.995	3.32(−2)	1.20(−7)
3.1623(−3)	302.6	2.425	2.245	3.32(−2)	1.20(−7)
1.7783(−3)	302.6	2.425	1.262	3.32(−2)	1.20(−7)
1.0000(−3)	302.6	2.425	7.096(−1)	3.32(−2)	1.20(−7)

* $N_2 = 0.78084 \times N$; $O_2 = 0.20948 \times N$.†Mixing ratios by volume; at all altitudes CH_4 mixing ratio = 1.6×10^{-6} ; H_2 mixing ratio = 5.5×10^{-7} .‡1.680(4) signifies 1.680×10^4 .

transport-kinetics equations where the time rate of change of species j is the sum of its chemical reaction rates and flux divergence, represented by eddy diffusion:

$$\frac{\partial}{\partial z} \left[K(z)N(z) \frac{\partial \chi_j(z, t)}{\partial z} \right] + P_j(z, t) - L_j(z, t) = \frac{\partial c_j(z, t)}{\partial t} \quad (1)$$

where z = altitude, t = time, $K(z)$ = eddy diffusion coefficient ($\text{cm}^2 \text{ s}^{-1}$), $N(z)$ = molecular density (cm^{-3}) of background air, $\chi_j(z, t)$ = mixing ratio or mole fraction of species j , $c_j(z, t)$ is concentration (cm^{-3}), $P_j(z, t)$, $L_j(z, t)$ = production, loss rates ($\text{cm}^{-3} \text{ s}^{-1}$) for chemical reaction of species j .

Our model of the marine boundary layer spans altitudes from 1 mm to 1 km, with 24 grid points and log-linear spacing between points (Table 1). The continuity equations are solved for 17 radicals and gaseous species (the predominant trace gases in the unpolluted marine troposphere): O_3 , $O(^3P)$, H , and the oxides of hydrogen (OH , HO_2 , H_2O_2), the oxides of nitrogen (NO , NO_2 , NO_3 , N_2O_5 , HNO_3 , HNO_4) and hydrocarbons resulting from methane oxidation (CH_3 , CH_3O , CH_3O_2 , CH_3O_2H , H_2CO). Fixed profiles based on measurements are assumed for CH_4 [Ehhalt, 1978], CO [Seiler, 1974], H_2 [Ehhalt et al., 1977], and H_2O [Valley, 1965]. Molecular densities and a tropical temperature profile (Table 1) are taken from U.S. Standard Atmosphere Supplements (1966) with modifications appropriate to a marine trade wind boundary layer [LeMone, 1980]. A detailed description of the basic chemical model is given in Thompson and Cicerone [1982]. Besides the modified altitude domain, the only change in model input since our earlier report is a rate constant revision according to the recent NASA [1982] recommendation. Marine boundary conditions have been chosen to yield calculated mixing ratios consistent with the low values (5–20 ppb

O_3 , 1–10 ppt NO_x , 20–80 ppt HNO_3) observed in the boundary layer [Routhier et al., 1980; McFarland et al., 1979; Huebert and Lazrus, 1980; Hélas and Warneck, 1981]. This is accomplished by specifying downfluxes of odd nitrogen species and ozone at the upper boundary and dry deposition at the lower boundary; for NO a surface upflux is also assumed in most model runs. Most other species are set at photochemical equilibrium. Photolysis rates used in (1) are calculated as described in Thompson [1984]. The overhead ozone column (sun-to-earth at local noon = 0.30 cm atm) is appropriate for summertime mid to low latitudes.

Transport

The model transport parameterization is based on the assumption that eddy diffusion $K(z)$ at height z can be represented in the boundary layer by

$$K(z, t) = u_* \kappa z [\phi_H(z/L, t)]^{-1} \quad (2)$$

where u_* (m s^{-1}) is the surface friction velocity, κ is the von Karman constant (0.35), and $\phi_H(z/L, t)$, which is the dimensionless temperature gradient, is a function of the stability parameter, z/L , with L the Monin-Obukhov length. We assume that $K(z)$ is not affected by chemical reactions and that the dimensionless gradient for mass transfer is equal to that of temperature and use the formulation of Businger et al. [1971] to evaluate ϕ_H :

$$\phi_H(z/L, t) = 0.74(1 - 9 z/L)^{-1/2} \quad z/L \leq 0 \quad (3)$$

The Monin-Obukhov length L is a function of the surface stress (via the friction velocity u_*), the buoyancy parameter g/\bar{T} , where g is gravitational acceleration and \bar{T} is mean tem-

perature, and surface virtual temperature flux, Q :

$$L = -\frac{u_*^3 \bar{T}}{\kappa g Q} \quad (4)$$

A positive temperature flux (z/L negative) signifies turbulence generation by buoyancy.

This parameterization is a first attempt at investigating the detailed structure of chemically reactive species near the surface. It is hoped that this will help pave the way to more accurate simulations using large eddy simulation models or more detailed parameterizations of the mixing process [Wyngaard and Brost, 1984; Wyngaard, 1984].

In this study we are interested in simulating the undisturbed tropical ocean where surface fluxes of heat, moisture, and momentum are small and relatively constant day and night. Thus, a steady state $K(z)$ can be reasonably assumed over a diurnal cycle. Equation (3) is used to evaluate $K(z)$ from 0.001 to 100 m with $L = -20$ m, an appropriate value for the atmospheric surface layer above the tropical ocean [LeMone, 1980]. We further assume $u_* = 0.15 \text{ m s}^{-1}$, which corresponds to a mean wind speed of about 4 m s^{-1} . We note that as we approach the surface, the stability effect on K becomes progressively smaller. For example, at $z = 0.05 L$, which corresponds to 1 m height in the case presented here, K is increased by 20% over its neutral value. Thus, near the surface the details of the species distributions are little affected by stability. Near the surface, the surface transfer length z_s [Hicks and Liss, 1976] also needs to be considered. The height above the surface is actually given by $z + z_s$, but hereinafter we refer to this height as z . Above the ocean, $z_s \sim 1 \text{ mm}$. The altitude dependence of K is shown in Figure 1; K values at model grid points are given in Table 1.

There are two reasons for choosing the lowest grid point so close to the surface (1 mm). First we want to resolve transport effects on chemistry on the scale of a few centimeters since this is the region in which chamber flux measurements of reactive species are obtained [Zafiriou and McFarland, 1981]. As shown in the appendix, we can also compare the model solution with an analytic solution for NO in the region close to the surface. We find that chemical reactivity significantly affects the concentration profile above $\sim 20 \text{ cm}$ height. Second, we want to calculate mixing ratios adjacent to the air-sea interface to test the validity of the thin film approximation for estimating air-sea fluxes of highly reactive species (e.g., NO) [Thompson and Zafiriou, 1983].

In the mixed layer above the surface layer (~ 100 – 550 m in the model) the expression suggested by Lamb and Durran [1978] is used to evaluate $K(z)$:

$$K(z) = 0.2 w_* z_i \quad (5)$$

where the convective velocity scale $w_* \equiv (Q z_i g / \bar{T})^{1/3}$ and z_i is the height of the mixed layer. The exact choice of K in the mixed layer is not critical. Model runs with K increased to $0.5 w_* z_i$ throughout the mixed layer showed no appreciable effect on chemical profiles. We take $z_i = 550 \text{ m}$ [LeMone, 1980] and assume, as in the surface layer, that $K(z)$ is time independent.

Across the top of the planetary boundary layer (PBL), we assume a discrete jump in concentration and calculate the fluxes, F_c , from the entrainment relation [Lilly, 1968]

$$F_c = -w_e \Delta c$$

where w_e is the entrainment velocity and Δc is the difference in concentration across the top of the boundary layer. We

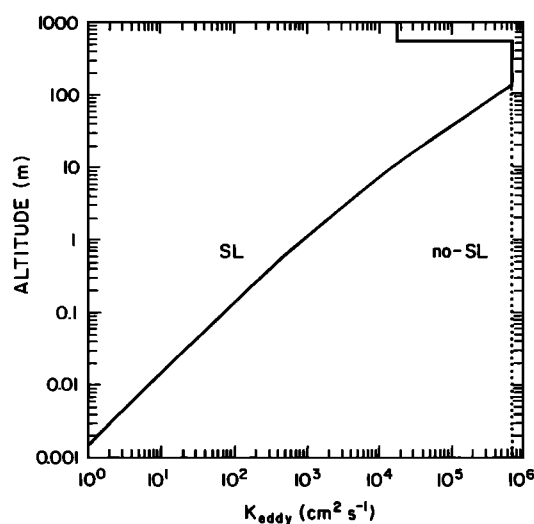


Fig. 1. Marine boundary layer transport. Solid line (SL model) includes parameterization of surface layer with slow diffusion near the surface. Dotted line (no-SL model) is identical to SL model except below 75 m. Planetary boundary layer (PBL), region of most efficient mixing, extends from 100 to 550 m.

assume a steady state horizontally homogeneous boundary layer, so that w_e is equal to minus the subsidence velocity. According to Albrecht [1979], a typical value for the subsidence velocity is 0.003 m s^{-1} . In the model, this is equivalent to specifying a value of $K = w_e \Delta z = 1.68 \times 10^4 \text{ cm}^2 \text{ s}^{-1}$ in the grid interval across the top of the boundary layer.

We have also extended the model, as a test, to 10 km height and used a range of values of K in the free troposphere with the same specified influx conditions, and found that in the boundary layer the model results are relatively insensitive to the diffusivity.

Equations (2)–(4) are based on similarity theory, which assumes that fluxes are constant throughout the surface layer. Lenschow [1982] has shown that (2) does not apply exactly to nonconserved species (e.g., those for which near-surface turbulence prevents photochemical equilibrium from being reached). Fitzjarrald and Lenschow [1983] have developed a modified flux-gradient relationship in the surface layer which we have applied in a test case to the diffusivity for NO. Their formulation is, at best, only an approximate correction for small deviations of K from its nonreactive value. We have, therefore, limited changes in K to $K/2 \leq K_{\text{NO}} \leq 2K$, where K_{NO} is the K modified by chemical reactions. The results indicate that the concentration of NO does not change by more than 10% throughout the surface layer. Fitzjarrald and Lenschow [1983] have also pointed out that the photostationary state is equivalent to having zero turbulent flux divergence and is in general only attainable at a single point in the surface layer. A coupled chemical-surface layer model is well suited for studying in more detail departures of the photostationary state due to turbulent transport.

3. RESULTS AND DISCUSSION

Background-Level Chemistry of the Marine Boundary Layer

This section presents typical results from simulations of the unpolluted boundary layer using the chemical and transport schemes described in the previous section. Illustrations have been chosen to emphasize differences between distributions

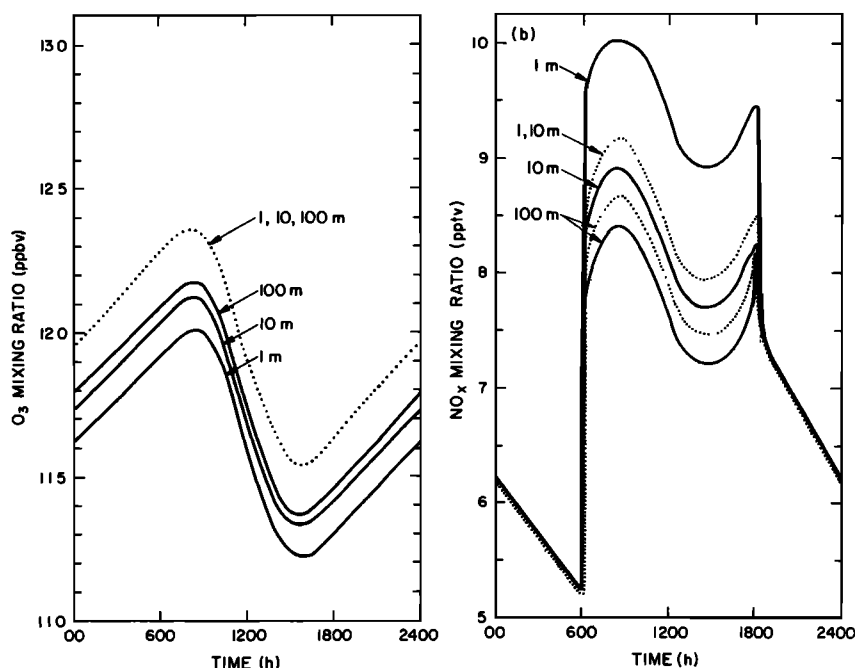
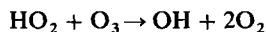
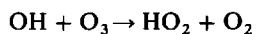


Fig. 2. Diurnal cycles of trace gases in boundary layer. (a) O_3 : Note distinction in mixing ratios between 1 and 10 m levels when model is used which specifies a surface layer parameterization (SL, solid lines). (b) NO_x ($=NO + NO_2$). Large gradient throughout surface layer in daytime (solid lines) results from surface (sea \rightarrow air) input of NO. At night NO_x decreases as NO_2 is converted to NO_3 : $NO_2 + O_3 \rightarrow NO_3 + O_2$.

calculated with the present model and those obtained using a model without a detailed treatment of the surface layer. Results of both diurnally averaged and time-dependent calculations are reported. All refer to converged diurnal behavior. By this we mean that the equations (1) are integrated until all species have attained a truly periodic 24-hour cycle. Diurnally averaged results are taken from averaged concentrations over the course of a converged diurnal model.

Figures 2a and 2b show the diurnal cycles (solid lines) of ozone and NO_x calculated at three levels. Two are chosen to represent conditions within the surface layer (1 and 10 m) and the third is in the mixed layer (100 m). Also shown in Figure 2 are diurnal cycles (dotted lines) calculated with large K ($10^5 - 10^6 \text{ cm}^2 \text{ s}^{-1}$ at the lowest grid points) extending to the surface. The latter, which we designate as "no-SL" transport, is the parameterization most commonly employed in previous photochemical transport-kinetics models. The diurnal behavior is similar in both cases. Ozone (Figure 2a) decreases slightly during daytime hours as a result of photochemical OH and catalytic loss by



The refined boundary layer results (SL model) reveal at all times of day a small O_3 gradient within the SL and mixing ratios throughout most of the surface layer which are different from those computed with no SL. Similarly for NO_x a substantial surface layer gradient is predicted by the SL model for daytime hours (600–1800 hours) when a surface NO upflux is assumed. Of course, diurnal averages calculated by the two schemes are different. This can be seen in Figure 3 where diurnally averaged vertical profiles of O_3 and NO_x (0.001–1000 m) are shown. Note curvature in the O_3 profile with the SL model compared to the no-SL profile (Figure 3a). We refer

to this phenomenon as a surface layer "bottleneck." The bottleneck effect on O_3 is fairly weak because O_3 is removed at a relatively small rate. For gases with large deposition velocities (e.g., HNO_3 , H_2O_2 , CH_3OOH , H_2CO) the bottleneck is more pronounced (see Figure 4 and discussion of HNO_3 below).

Odd Nitrogen Chemistry in the Surface Layer

Thompson and Cicerone [1982] noted that model calculations of odd nitrogen are very sensitive to assumed transport, boundary conditions, and simulated episodes of clouds and precipitation. For example, when a small diffusivity ($K \sim 10^3 \text{ cm}^2 \text{ s}^{-1}$) is assumed in the surface layer, an NO upflux gives a significant gradient of NO and variable NO/ HNO_3 throughout the surface boundary layer. Washout of HNO_3 by precipitation may produce large variability in NO/ HNO_3 on a short time scale. A related study [Thompson and Zafriou, 1983] showed that the ratio NO/ HNO_3 can be affected by aerosol scavenging of HNO_3 , which typically partitions the majority of near surface HNO_3 as particulate nitrate [Huebert, 1980; Savoie and Prospero, 1982]. In this section results from the refined boundary layer model are used to examine some of these phenomena in more detail. The reason for doing so are to compare calculations with an existing marine O_3 , NO, and HNO_3 data set [Liu et al., 1983, and references therein] and to suggest scenarios for further measurements in the unpolluted marine troposphere. In this connection we have also examined the NO- NO_2 - O_3 photostationary state relationship in the SL.

Figure 4 shows vertical profiles of NO and HNO_3 at noon-time calculated from three model simulations. An identical odd nitrogen upper boundary condition applies to all three cases, but transport and lower boundary assumptions vary. The dashed profile is taken from model runs in which both

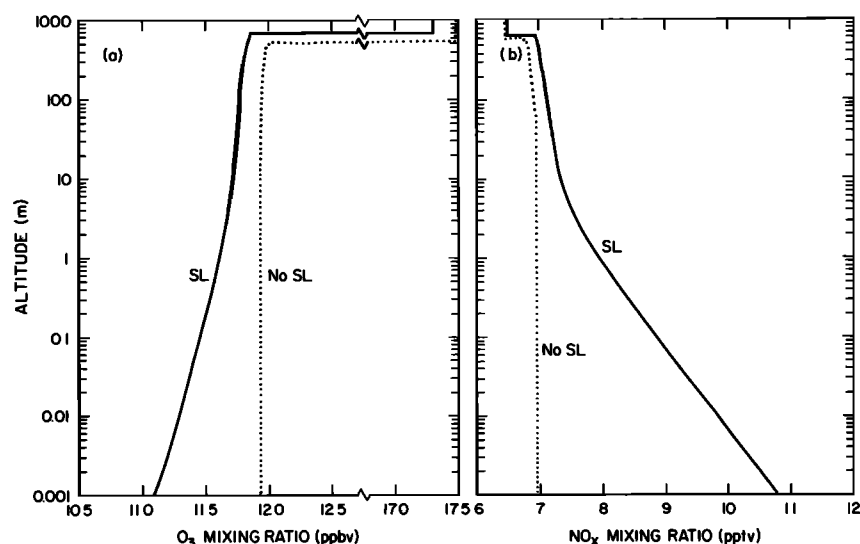


Fig. 3. Diurnally averaged mixing ratio profiles with SL and no-SL models: (a) O_3 ; (b) NO_x . Discontinuities at PBL-free troposphere interface result from assumed entrainment rate and upper boundary fluxes. Free troposphere mixing ratios compare well with data [Routhier *et al.*, 1980; B. A. Ridley, personal communication, 1984]. NO_x calculated in the free troposphere is less than in the boundary layer because the relatively high free troposphere O_3 (and OH) convert much of the NO_x to HNO_3 . Total odd nitrogen ($NO_x + HNO_3 + HNO_4 + NO_3 + N_2O_5$) is higher in the free troposphere than in the boundary layer as required by specification of an odd nitrogen influx at the upper boundary.

HNO_3 and NO are removed at the surface (deposition velocities based on a reference height of 1 m = 0.43 cm s^{-1} and $0.00017 \text{ cm s}^{-1}$, respectively [Thompson and Zafiriou, 1983]). In fact, the low removal velocity of NO is nearly equivalent to a specification of photochemical equilibrium for NO at the lower boundary. The solid profile is taken from a calculation with distinct SL transport in which an NO sea-to-air flux = $1.5 \times 10^8 \text{ cm}^{-2} \text{ s}^{-1}$ is prescribed throughout model daytime (12 hours). The dotted profile assumes the same NO upflux but uses the no-SL transport model (i.e., fixed, rapid eddy diffusion in the surface layer (cf. Figures 2 and 3)). Also shown in Figure 4 is the mean midday mixing ratio of NO [McFarland *et al.*, 1979] and Huebert's [1980] mean HNO_3 mixing ratio (no rain conditions) measured on the 1978 Knorr 73/7 cruise. These are indicated at 10 m which is roughly ship height. The McFarland *et al.* [1979] NO values are similar to those of Noxon [1981] and to Hélas and Warneck's [1981] measurements of NO_x made on an Atlantic Ocean Europe-to-South America cruise track (Meteor, 1980). As a group, these data suggest that a few parts per trillion NO is typical of the remote marine surface troposphere. Mixing ratios calculated with an NO upflux compare favorably with the NO data, whereas without the NO source the calculated mixing ratio at 10 m is a factor of ~ 5 too low. The specified upflux in the model, $1.5 \times 10^8 \text{ cm}^{-2} \text{ s}^{-1}$, is close to Zafiriou and McFarland's [1981] estimate of NO upwelling during the Knorr cruise, $1.3 \times 10^8 \text{ cm}^{-2} \text{ s}^{-1}$. Note that the 1 mm NO mixing ratio, 9 pptv, although much greater than the ship height value used by Zafiriou and McFarland [1981] to estimate the sea-to-air flux, is still insignificant compared to dissolved NO , equivalent gas-phase mixing ratio ~ 30 ppbv. Thus, it is valid to use a two-layer thin film model to estimate air-sea fluxes of reactive species throughout the surface layer. It appears from Figure 4 that on the Knorr cruise the oceanic NO source may have been controlling NO_x in the surface layer. This does not exclude the importance of other sources in controlling the overall odd nitrogen budget in the remote marine boundary

layer. Liu *et al.* [1983] have noted that the total amount of odd nitrogen measured on the Knorr cruise (75% was particulate nitrate) would require an input equivalent to $\sim 10^9 \text{ cm}^{-2} \text{ s}^{-1}$, greatly in excess of the oceanic NO source. Our calculations give a similar result. One possibility for the missing source is lightning-derived NO [Liu *et al.*, 1983]. This could be included in our model by specifying a large odd nitrogen influx at the upper boundary.

Figure 4 (solid line) shows a significant NO gradient in the

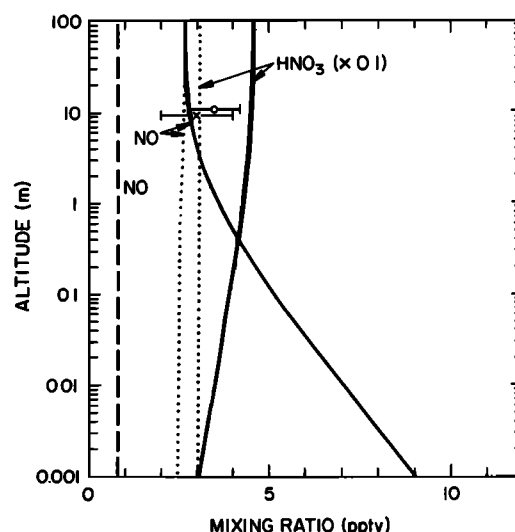


Fig. 4. Noontime mixing ratios of NO and HNO_3 in the surface layer (1 mm to 100 m). Three model calculations are illustrated: solid line, SL- NO flux = $1.5 \times 10^8 \text{ cm}^{-2} \text{ s}^{-1}$; dotted line, no SL- NO flux; dashed line, SL-no NO flux. Symbols at 10 m level represent ship-based measurements in the Equatorial Pacific from the Knorr 73/7 cruise in 1978; circle, NO , midday values [McFarland *et al.*, 1979]; cross, HNO_3 [Huebert, 1980]. The HNO_3 value is a mean of seven measurements not taken during rain shower conditions. The ranges shown for the data correspond to 1σ .

TABLE 2. Ratio, $[\text{NO}]/[\text{HNO}_3]$ at noontime, in Surface Layer

Altitude, m	SL Model	No-SL Model
100	0.057	0.086
10	0.063	0.088
1	0.085	0.085
0.1	0.13	0.082
0.01	0.20	0.081
0.001	0.30	0.081

NO Upflux = $1.5 \times 10^8 \text{ cm}^{-2} \text{ s}^{-1}$, daytime.

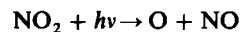
SL as a result of slow upward mixing and loss of NO by chemical reaction. Between the surface (1 mm in the model) and 1 m NO falls off 60% and between 1 and 10 m it diminishes another 22%. In response to the NO forcing the corresponding NO_2 profile also shows a negative gradient away from the surface. The HNO_3 gradient (solid line) is positive away from the surface—a response to the SL bottleneck—and the ratio NO/HNO_3 varies from 30 to 6% between 1 mm and 10 m (Table 2). These results demonstrate that gradients must be taken into account when interpreting field measurements of odd nitrogen species and ozone near the surface. Surface emission of NO can be estimated by measuring its concentration (as well as those of NO_2 and O_3) at several levels in the surface layer and then solving for the surface flux by the method discussed by Fitzjarrald and Lenschow [1983]. The loss of NO by chemical reactions increases the gradient of NO near the surface and thus increases the sensitivity of the profile method for estimating surface emission. In the appendix we show that in the surface layer the NO continuity equation (1) can be approximated by a form which yields an analytic solution for NO concentrations. Note that the gradients do not appear in results from a model which assumes rapid uniform diffusion throughout the surface layer (Figure 4, dotted lines, and Table 2).

We note that in most situations in the marine environment aerosol interaction with HNO_3 is likely to be a more important influence than turbulence on NO/HNO_3 . Removal of HNO_3 vapor to particles decreases the mixing ratio relative to a no-aerosol environment and forms nitrate in particles [Martens *et al.*, 1973; Huebert, 1980; Savoie and Prospero, 1982]. In Thompson and Zafiriou [1983] we found that including aerosol scavenging in model simulations reduces surface HNO_3 to about one third of its no-aerosol value. Although the parameterization of aerosol removal in that study was very rough, the implication that particulate nitrate is ~ 3 times greater than vapor phase HNO_3 is consistent with Huebert's vapor and particulate nitrate measurement on the Knorr 73/7 cruise [Huebert, 1980; Liu *et al.*, 1983]. A threefold reduction of surface gaseous HNO_3 in the current model implies a threefold increase in NO_x/HNO_3 , since NO_x is not directly affected by the aerosol. We note, however, that gas-aerosol partitioning depends on particle size distributions which may vary both temporally and spatially throughout the SL. The complexity of these phenomena makes it difficult to model aerosol effects on HNO_3 quantitatively. It suffices here to point out that we have indicated a likely sensitivity level of SL HNO_3 to aerosol scavenging. A more accurate calculation of HNO_3 -particulate interaction must account for the complex dynamics of gas-particle interactions; this is a task that is beyond the scope of this paper.

The photostationary ratio, R_{ps} , is evaluated from

$$R_{ps} = \frac{k_6[\text{NO}][\text{O}_3]}{J_{\text{NO}_2}[\text{NO}_2]} \quad (6)$$

where k_6 and J_{NO_2} are the rates of reactions $\text{NO} + \text{O}_3 \rightarrow \text{NO}_2 + \text{O}_2$ and $\text{NO}_2 + h\nu \rightarrow \text{NO} + \text{O}$, respectively. R_{ps} is a measure of the degree to which the O_3 , NO_2 , and NO budgets are governed only by these two reactions. The first one represents O_3 loss and the second is the effective rate of O_3 formation through its rate-determining role in the sequence:



Analysis of field measurements shows that in the atmosphere R_{ps} often deviates from unity [Kelly *et al.*, 1980; Shetter *et al.*, 1983]. Both positive, $R_{ps} > 1$, and negative deviations, $R_{ps} < 1$, have been observed. Calvert and Stockwell [1983] have analyzed the photochemistry of ozone to derive a more complete expression than (6) for the photostationary ratio. For the unpolluted troposphere considered here (negligible olefin reaction with O_3) the ratio is given by

$$\begin{aligned} R_{ps} &= \frac{k_6[\text{NO}][\text{O}_3]}{J_{\text{NO}_2}[\text{NO}_2]} \\ &= \left\{ 1 + \frac{1}{k_6[\text{NO}]} \left[\frac{k_{13}[\text{O}(\text{D})][\text{H}_2\text{O}]}{[\text{O}_3]} + k_8[\text{NO}_2] \right. \right. \\ &\quad \left. \left. + k_{19}[\text{OH}] + k_{20}[\text{HO}_2] + \frac{1}{[\text{O}_3]} \frac{d[\text{O}_3]}{dt} \right. \right. \\ &\quad \left. \left. + \frac{1}{[\text{O}_3]} FD_{\text{O}_3} \right] \right\}^{-1} \quad (7) \end{aligned}$$

Reaction numbers are explained in Table 3. The ozone flux divergence, $[FD_{\text{O}_3}]$ in (7), which does not appear in Calvert and Stockwell's [1983] box model formulation, is represented in a one-dimensional model by the first term in (1). Thus, transport as well as chemical reactions can affect the photostationary ratio.

We have examined both temporal and spatial variation of the photostationary ratio using model-derived mixing ratios of NO, NO_2 , and O_3 to compute R_{ps} in (6). Figure 5 shows R_{ps} at the 1 m level, over the course of model daytime (600–1800 hours). Near sunrise there are large positive deviations in R_{ps} . As the model day advances R_{ps} decreases, reaching a minimum value (~ 0.5) at noon and increasing again in the afternoon. Evaluation of the individual terms in (7) (right-hand side) gives insight into causes for the nonunity value of R_{ps} . Table 3 presents the dominant terms in (7) and the resulting R_{ps} .

When there is a significant gradient of NO_x and O_3 (as in the NO upflux-SL) model, R_{ps} has a considerable vertical gradient. Figure 6 shows noontime R_{ps} in the surface layer calculated from (6) for the two NO upflux cases (SL, solid line; no SL, dotted line). R_{ps} at 1 mm is 2.8 times larger than the 10 m value. The reason for this is that NO injected at the surface increases $k_6[\text{NO}]$, and consumes ozone to give a smaller O_3 surface flux. The latter response is not quantitative and the net result is a relative increase in $k_6[\text{NO}]$ relative to its multiplier in (7). This causes R_{ps} near the surface to be greater than just above it. As the NO gradient diminishes, R_{ps} decreases also. At 10 m the gradient is virtually gone and NO is close to the value it has in the no-SL model (see Figure 4). R_{ps} is nearly the same in both cases (cf. solid and dotted lines in Figure 6).

Figure 6 is a good illustration of micrometeorological and

TABLE 3. Analysis of the Surface Layer Photostationary Ratio, Noontime

Altitude, m	$[\text{O}_3]\Sigma^*$, $\text{cm}^{-3} \text{s}^{-1}$	$\frac{d[\text{O}_3]}{dt}$, $\text{cm}^{-3} \text{s}^{-1}$	FD_{O_3} , $\text{cm}^{-3} \text{s}^{-1}$	$[\text{O}_3]\Sigma + \frac{d[\text{O}_3]}{dt}$, $(\text{cm}^{-3} \text{s}^{-1}) + \text{FD}_{\text{O}_3}$	$k_6[\text{NO}][\text{O}_3]$, $\text{cm}^{-3} \text{s}^{-1}$	calc† R_{ps}
10^2	2.3 (6)‡	-1.4 (6)	-4.0 (5)	5.2 (5)	3.5 (5)	0.40
10	2.3 (6)	-1.4 (6)	-3.2 (5)	5.6 (5)	3.7 (5)	0.41
1.0	2.3 (6)	-1.4 (6)	-3.5 (5)	5.2 (5)	4.9 (5)	0.48
0.1	2.3 (6)	-1.4 (6)	-5.0 (5)	3.5 (5)	7.0 (5)	0.66
0.01	2.2 (6)	-1.4 (6)	-7.2 (5)	1.2 (5)	9.5 (5)	0.89
0.001	2.2 (6)	-1.3 (6)	-9.6 (5)	-1.4 (5)	1.2 (6)	1.13

* $\Sigma = \frac{k_{13}[\text{O}(^1D)][\text{H}_2\text{O}]}{[\text{O}_3]} + k_{19}[\text{OH}] + k_{20}[\text{HO}_2] + k_8[\text{NO}_2]$; Rate constants are for processes: k_{13} , $\text{O}(^1D) + \text{H}_2\text{O} \rightarrow 2\text{OH}$; k_{19} , $\text{OH} + \text{O}_3 \rightarrow \text{HO}_2 + \text{O}_2$; k_{20} , $\text{HO}_2 + \text{O}_3 \rightarrow \text{OH} + 2\text{O}_2$; k_8 , $\text{NO}_2 + \text{O}_3 \rightarrow \text{NO}_3 + \text{O}_2$.

$$\dagger R_{ps}^{\text{calc}} = \left\{ 1 + \frac{1}{k_6[\text{NO}]} \left(\Sigma + \frac{1}{[\text{O}_3]} \frac{d[\text{O}_3]}{dt} + \frac{1}{[\text{O}_3]} \text{FD}_{\text{O}_3} \right) \right\}^{-1}.$$

‡2.3(6) signifies 2.3×10^6 .

chemical influences on the photostationary ratio. This can be seen by looking at Table 3 where R_{ps} of Figure 6 is presented along with the individual terms of (7). Throughout the surface layer $d\text{O}_3/dt$ and the summed chemical loss terms, Σ ,

$$\Sigma = \frac{k_{13}[\text{O}(^1D)][\text{H}_2\text{O}]}{[\text{O}_3]} + k_{19}[\text{OH}] + k_{20}[\text{HO}_2] + k_8[\text{NO}_2]$$

are nearly constant, whereas FD_{O_3} varies greatly. At one point, ~ 3 mm, the sum of the terms in (7) multiplied by $1/k_6[\text{NO}]$ is zero and $R_{ps} = 1$. Away from the surface, FD_{O_3} decreases and R_{ps} approaches a constant value (~ 0.40), very different from unity. We call this asymptotic value a chemical pseudo-photostationary ratio

$$R_{pps} = R_{ps, \text{asymptotic}}$$

In other words, R_{pps} is the photostationary ratio defined by transport and photochemistry well above the region in which surface layer chemical and turbulent effects are varying rapidly with altitude. R_{pps} is much different from unity because the chemical mechanism controlling ozone is more compli-

cated than that implied by the two reactions defining (6). Micrometeorological disturbances to the photostationary ratio are apparent in deviations from R_{pps} . In our model simulations (Figure 6) these deviations are evident in the lowest few meters where the NO upflux forces the values of R_{ps} away from R_{pps} . Since calculated mixing ratios of NO and O_3 are similar to those measured in the remote marine troposphere, the photostationary ratio characteristics described here should be observed in such environments.

4. SUMMARY AND CONCLUSIONS

We have presented a one-dimensional photochemical transport-kinetics model which employs a very fine vertical grid with eddy diffusion as formulated by *Businger et al.* [1971] to simulate the marine surface boundary layer (SL model). Chemical species and radiation specified in the model apply to the remote tropical troposphere (low NO_x , low O_3 , high H_2O vapor). General model features of odd nitrogen and ozone chemistry have been described and compared to results from a model without a distinct surface layer parameterization. Gradients of rapidly depositing species (e.g., HNO_3 , H_2CO , H_2O_2) and surface injected NO are more pronounced in the SL model.

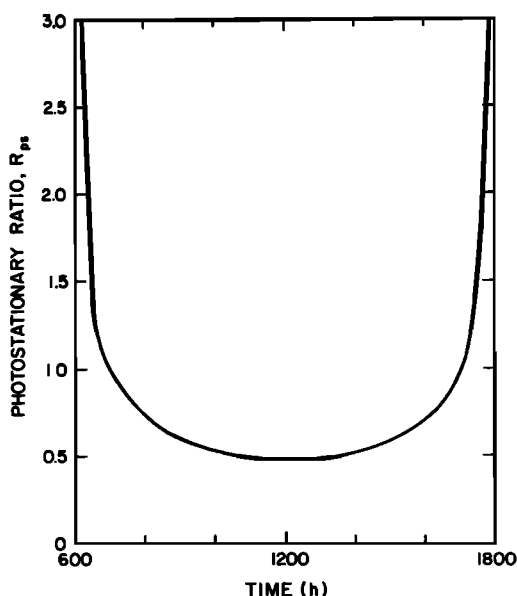


Fig. 5. The photostationary state ratio, $R_{ps} = k_6[\text{NO}][\text{O}_3]/J_{\text{NO}_2}[\text{NO}_2]$, at 1 m, as function of time of day.

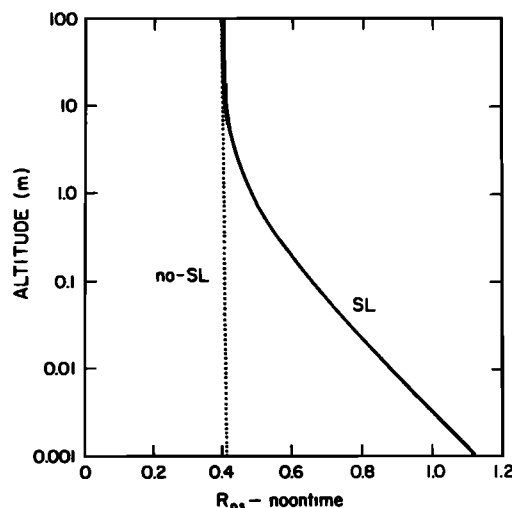


Fig. 6. Photostationary state ratio at 1200 hours in the surface and mixed layers. An NO upflux ($1.5 \times 10^8 \text{ cm}^{-2} \text{ s}^{-1}$) is assumed in model calculations. Solid line, SL model; dotted line, no-SL model.

A comparison of model results with NO, HNO₃, and O₃ data measured in the Equatorial Pacific (*Knorr 73/7*) shows good agreement and suggests that oceanic NO upwelling controlled surface layer NO_x during that cruise. Total gas and particulate HNO₃ measured on the *Knorr* cruise was higher than our model gas-phase HNO₃, however, and a large nonlocal odd nitrogen source is required to balance the total odd nitrogen budget [*Liu et al., 1983*].

Model calculations of the NO-NO₂-O₃ photostationary ratio, R_{ps} , show considerable vertical gradient when an oceanic NO upflux is assumed. Throughout most of the model domain $R_{ps} < 1$. Analysis of the photostationary equation reveals that there are both micrometeorological and chemical contributions to R_{ps} . The concept of a pseudo-photostationary ratio R_{pps} is introduced to distinguish between situations in which one or the other factor is dominant. This rate is defined as the asymptotic value approached above the SL where theory [*Fitzjarrald and Lenschow, 1983*] predicts photochemical equilibrium should be attainable for fast chemical reactions. Both diffusion and chemical reactions involving O₃ determine R_{pps} . At noon in the remote troposphere R_{pps} is ~0.4. Near surface turbulence combined with an NO upflux pushes the photostationary state value at 1 mm up to 1.1.

In conclusion we emphasize that our analysis of the *Knorr 73/7* data is not meant to be definitive. On the other hand, neither do we suppose that the chemical characteristics of the boundary layer described are unusual for synoptically undisturbed situations in which the ocean is emitting NO. More generally, we have presented our model as a complement to coarser grid models to illustrate the usefulness of a refined transport scheme in investigating chemically reactive species in the surface layer. We hope that the results clarify sensitivities of odd nitrogen and the NO-NO₂-O₃ photostationary ratio in the marine surface layer and stimulate further measurements.

APPENDIX

The continuity equation for a rapidly reacting species in the surface layer (equation (1)) can be solved approximately by an analytical method. We illustrate this method by applying it to NO. Consider the following:

$$\frac{\partial c_{NO}}{\partial t} = \frac{\partial}{\partial z} \left(KN \frac{\partial \chi_{NO}}{\partial z} \right) + P_{NO} - L_{NO} \quad (A1)$$

Throughout model daytime (except near sunrise and sunset), $\partial c_{NO}/\partial t$ is essentially zero. In the lower surface layer, $z = 1$ mm to $z = 10$ m, N is virtually constant. For these conditions, (A1) may be rewritten

$$\frac{d}{dz} \left(K \frac{dc_{NO}}{dz} \right) + P_{NO} - R_{NO}c_{NO} = 0 \quad (A2)$$

where $c_{NO} = \chi_{NO}N$ and R_{NO} is the sum of all NO loss reactions written as a first-order process. Close to the surface a good approximation to the eddy diffusion is $K(z) \cong \kappa u_* z / 0.74$ (equations (2) and (3)). Then (A2) can be rewritten

$$z \frac{d^2 c_{NO}}{dz^2} + \frac{dc_{NO}}{dz} - \frac{0.74 R_{NO} c_{NO}}{\kappa u_*} = -\frac{0.74 P_{NO}}{\kappa u_*} \quad (A3)$$

Letting $l = \kappa u_* / 0.74 R_{NO}$, $P = 0.74 P_{NO} / \kappa u_*$, and $y = c_{NO} - Pl$, we obtain from (A3):

$$z \frac{d^2 y}{dz^2} + \frac{dy}{dz} - \frac{y}{l} = 0 \quad (A4)$$

From 1 mm to 1 m, P varies ~15%, l varies less than 10%; we assume for simplicity that they are constant. The solution to (A4) is a sum of zero-order modified Bessel functions [*Abramowitz and Stegun, 1965*]:

$$y(z) = c_{NO}(z) - Pl = AK_0 \left(2 \sqrt{\frac{z}{l}} \right) + BI_0 \left(2 \sqrt{\frac{z}{l}} \right) \quad (A5)$$

where A and B are constants. For this case, B is zero since c_{NO} approaches a constant value as z increases. The constant A is evaluated from the lower boundary condition. Calling the lowest point in the model z_{LB} , we want to evaluate

$$\left[\frac{dc_{NO}}{dz} \right]_{z_{LB}} = -A \sqrt{\frac{1}{z_{LB}l}} K_1 \left(2 \sqrt{\frac{z_{LB}}{l}} \right) \quad (A6)$$

In (A6) dc_{NO}/dz is obtained from $K(z_{LB}) \cong \kappa u_* z_{LB} / 0.74$ and the flux $F_{NO} = 1.5 \times 10^8 \text{ cm}^{-2} \text{ s}^{-1}$ [*Lenschow, 1982*]:

$$\left[\frac{dc_{NO}}{dz} \right]_{z_{LB}} = -\frac{F_{NO}}{K(z_{LB})} \quad (A7)$$

Model-calculated chemical production, $P_{NO}(z)$, and losses, $R_{NO}(z)$, are used to evaluate P , l , and Pl . At model noontime Pl varies from $8.0 \times 10^7 \text{ cm}^{-3}$ at 1 mm to $6.5 \times 10^7 \text{ cm}^{-3}$ at 10 m. The most physically reasonable value to use in (A5) is one which pertains to the largest part of the surface layer (e.g., from 1 to 10 m). We use an average of Pl values in the 1–10 m range: $6.61 \times 10^7 \text{ cm}^{-3}$. At 1200 hours the solution to (A3) (in cm^{-3}) is

$$c_{NO}(z) = y(z) + Pl = 4.23 \times 10^7 K_0 \left(2 \sqrt{\frac{z}{l}} \right) + 6.61 \times 10^7 \quad (A8)$$

Figure A1 (solid line) illustrates c_{NO} evaluated from $z = 1$ mm to $z = 10$ m. The model-derived noontime NO profile is also shown (dashed line). The two curves are in very good agree-

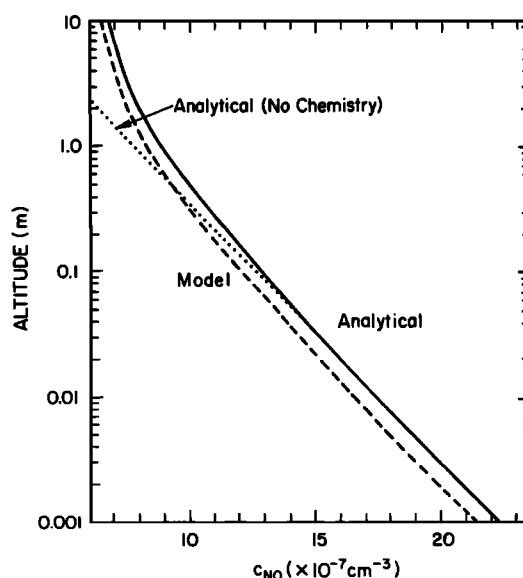


Fig. A1. NO number density at noontime, c_{NO} , as a function of altitude in the surface layer. The solid line represents the analytical solution (equation (A8)) to an approximate continuity equation. The dashed profile was obtained from the model solution to (A1). The dotted line is the analytical solution for a nonreactive species assuming a steady state concentration at $z = 0.1$ cm equal to the analytical reactive solution.

ment considering that great simplification went into the formulation of (A4) and that the model solves the continuity equation (A1) using interval-averaged $K(z)$ rather than $K(z)$ corresponding to the grid points. We also show, for comparison, the analytical solution for a nonreactive species using the concentration at z_{LB} as a boundary condition. We see that the NO concentration already begins to deviate significantly from the nonreactive solution at $z \cong 0.2$ m. Note that the analytical no chemistry solution is not the one which would be obtained with the model if there were no chemical reactions involving NO throughout the boundary layer; for this case mean NO would continue to increase in time and would not reach a steady state. Rather the nonreactive solution is for an assumed steady state concentration near the surface equal to that obtained from the analytic solution with chemical reactions. At 10 m agreement between the model and analytical solutions is good even though the basic assumption of the analytical approximation, namely that $K(z)$ is simply proportional to z (equation (A3)), is strictly valid only at the smallest values of z . This is because the predominant contribution to c_{NO} at 10 m is Pl (equation (A8)) rather than $AK_0(2\sqrt{z/l})$ which diminishes rapidly with z .

Acknowledgments. A.M.T. thanks NCAR for the Advanced Study Program Fellowship which supported this research. We thank John C. Wyngaard and William Stockwell for comments on the manuscript. We are grateful to Leif Kristensen of Risø National Laboratory, Denmark, for assistance with mathematical analysis and to Stacy Walters for programming assistance. The National Center for Atmospheric Research is sponsored by the National Science Foundation.

REFERENCES

- Abramowitz, M., and I. A. Stegun, *Handbook of Mathematical Functions, with Formulas, Graphs, and Mathematical Tables*, Dover, New York, p. 374, 1965.
- Albrecht, B. A., A model of the thermodynamic structure of the trade wind boundary layer, II, Applications, *J. Atmos. Sci.*, **36**, 90–98, 1979.
- Businger, J. A., J. C. Wyngaard, Y. Izumi, and E. F. Bradley, Flux-profile relationships in the atmospheric surface layer, *J. Atmos. Sci.*, **28**, 181–189, 1971.
- Calvert, J. G., and W. R. Stockwell, Deviations from the O_3 -NO- NO_2 photostationary state in tropospheric chemistry, *Can. J. Chem.*, **61**, 983–991, 1983.
- Chameides, W. L., D. H. Stedman, R. R. Dickerson, D. W. Rusch, and R. J. Cicerone, NO_x production in lightning, *J. Atmos. Sci.*, **34**, 143–149, 1977.
- Chatfield, R. B., and P. J. Crutzen, Sulfur dioxide in remote oceanic air: cloud transport of reactive precursors, *J. Geophys. Res.*, in press, 1984.
- Ehhalt, D. H., The CH_4 concentration over the ocean and its possible variation with latitude, *Tellus*, **30**, 169–176, 1978.
- Ehhalt, D. H., U. Schmidt, and L. E. Heidt, Vertical profiles of molecular hydrogen in the troposphere and stratosphere, *J. Geophys. Res.*, **82**, 5907–5911, 1977.
- Fitzjarrald, D. R., and D. H. Lenschow, Mean concentration and flux profiles for chemically reactive trace species in the atmospheric surface layer, *Atmos. Environ.*, **17**, 2505–2512, 1983.
- Gidel, L. T., Cumulus cloud transport of transient tracers, *J. Geophys. Res.*, **88**, 6587–6599, 1983.
- Hélas, G., and P. Warneck, Background NO_x mixing ratios in air masses over the North Atlantic Ocean, *J. Geophys. Res.*, **86**, 7283–7290, 1981.
- Hicks, B. B., and P. S. Liss, Transfer of SO_2 and other reactive gases across the air-sea interface, *Tellus*, **28**, 348–354, 1976.
- Huebert, B. J., Nitric acid and aerosol nitrate measurements in the Equatorial Pacific region, *Geophys. Res. Lett.*, **7**, 325–328, 1980.
- Huebert, B. J., and A. L. Lazrus, Tropospheric gas-phase and particulate nitrate measurements, *J. Geophys. Res.*, **85**, 7322–7328, 1980.
- Kelly, T. J., D. H. Stedman, J. A. Ritter, and R. B. Harvey, Measurements of oxides of nitrogen and nitric acid in clean air, *J. Geophys. Res.*, **85**, 7417–7425, 1980.
- Lamb, R. G., and D. R. Durran, Eddy diffusivities derived from a numerical model of the convective boundary layer, *Nuovo Cimento*, **1**, 1–17, 1978.
- LeMone, M. A., The marine boundary layer, in *Workshop on the Planetary Boundary Layer: 14–18 August 1978*, Boulder, Colo., edited by J. C. Wyngaard, American Meteorological Society, Boston, Mass., 1980.
- Lenschow, D. H., Reactive trace species in the boundary layer from a micrometeorological perspective, *J. Meteorol. Soc. Jpn.*, **60**, 472–480, 1982.
- Lilly, D. K., Models of cloud-topped mixed layers under a strong inversion, *Q. J. R. Meteorol. Soc.*, **92**, 292–309, 1968.
- Liu, S.-C., M. McFarland, D. Kley, O. Zafiriou, and B. Huebert, Tropospheric NO_x and O_3 budgets in the Equatorial Pacific, *J. Geophys. Res.*, **88**, 1360–1368, 1983.
- Martens, C. S., J. J. Wesolowski, R. C. Harriss, and R. Kaifer, Chlorine loss from Puerto Rican and San Francisco Bay area marine aerosols, *J. Geophys. Res.*, **78**, 8778–8792, 1973.
- McFarland, M., D. Kley, J. W. Drummond, A. L. Schmeltekopf, and R. J. Winkler, Nitric oxide measurements in the Equatorial Pacific region, *Geophys. Res. Lett.*, **6**, 605–608, 1979.
- NASA, Chemical kinetics and photochemical data for use in stratospheric modeling, *Eval. Number 5*, JPL Publ. 82-57, Jet Propul. Lab., Pasadena, Calif., 1982.
- Noxon, J. F., Atmospheric nitrogen fixation by lightning, *Geophys. Res. Lett.*, **3**, 463–465, 1976.
- Noxon, J. F., NO_x in the mid-Pacific troposphere, *Geophys. Res. Lett.*, **8**, 1223–1226, 1981.
- Routhier, F., R. Dennett, D. D. Davis, A. Wartburg, P. Haagenson, and A. C. Delany, Free tropospheric and boundary-layer airborne measurements of ozone over the latitude range of 58°S to 70°N, *J. Geophys. Res.*, **85**, 7307–7321, 1980.
- Savoie, D. L., and J. M. Prospero, Particle size distribution of nitrate and sulfate in the marine atmosphere, *Geophys. Res. Lett.*, **9**, 1207–1210, 1982.
- Seiler, W., The cycle of atmospheric CO, *Tellus*, **26**, 117–135, 1974.
- Shetter, R. E., D. H. Stedman, and D. H. West, The $NO/NO_2/O_3$ photostationary state in Claremont, California, *J. Air Pollut. Contr. Assn.*, **33**, 212–214, 1983.
- Thompson, A. M., The effect of clouds on photolysis rates and ozone formation in the unpolluted troposphere, *J. Geophys. Res.*, **89**, 1341–1349, 1984.
- Thompson, A. M., and R. J. Cicerone, Clouds and wet removal as causes of variability in the trace-gas composition of the marine troposphere, *J. Geophys. Res.*, **87**, 8811–8826, 1982.
- Thompson, A. M., and O. C. Zafiriou, Air-sea fluxes of transient atmospheric species, *J. Geophys. Res.*, **88**, 6696–6708, 1983.
- Valley, S. (ed.), *Handbook of Geophysics and Space Environments*, Chap. 3, McGraw-Hill, New York, 1965.
- Wyngaard, J. C., Toward convective PBL parameterization: a scalar transport module, *J. Atmos. Sci.*, **41**, 102–112, 1984.
- Wyngaard, J. C., and R. A. Brost, Top-down and bottom-up diffusion in the convective boundary layer, *J. Atmos. Sci.*, in press, 1984.
- Zafiriou, O. C., and M. McFarland, Nitric oxide from nitrate photolysis in the central Equatorial Pacific, *J. Geophys. Res.*, **86**, 3173–3182, 1981.
- Zafiriou, O. C., McFarland, M., and R. H. Bromund, Nitric oxide in seawater, *Science*, **207**, 637–639, 1980.

D. H. Lenschow and A. M. Thompson, National Center for Atmospheric Research, Boulder, CO 80307.

(Received November 17, 1983;
revised February 9, 1984;
accepted February 16, 1984.)